12-21-2007

Arabian Sea Response to Monsoon Variations

Raghu Murtugudde
University of Maryland, ragu@essic.umd.edu

Richard Seager
Columbia University

Prasad Thoppil
University of Southern Mississippi

Arabian Sea response to monsoon variations

Raghu Murtugudde,[1] Richard Seager,[2] and Prasad Thoppil[3]

Received 9 April 2007; revised 14 September 2007; accepted 4 October 2007; published 21 December 2007.

[1] This study aims to quantify the impact of strong monsoons on the mixed layer heat budget in the Arabian Sea by contrasting forced ocean general circulation model simulations with composite strong and weak monsoon winds. Strong (weak) monsoons are defined as years with zonal component of the Somali Jet being greater (smaller) by more than a standard deviation of the long-term mean of the National Centers for Environmental Prediction reanalysis winds. Coastal upwelling is shown to be demonstrably stronger for strong monsoons leading to significant surface cooling, shallower thermoclines, and deeper mixed layers. A coupled ecosystem model shows that surface chlorophyll, primary, and export production are indeed higher for strong monsoons compared to weak monsoons driven by the supply of colder, nutrient-rich waters from greater than 100 m depths. The surprising result is that a strong monsoon results in stronger negative wind stress curl away from the coasts and drives Ekman pumping that results in a deeper thermocline. The weaker stratification and larger turbulent kinetic energy from the winds drive deeper mixed layers leading entrainment cooling with some contribution from the advection of colder upwelled waters from the coastal upwelling regions. Thus the strong monsoons, in fact, enhance oceanic heat uptake indicating that ocean dynamics are cooling the surface and driving the lower atmosphere which has implications for the interpretation of monsoon variability from paleorecords.

Citation: Murtugudde, R., R. Seager, and P. Thoppil (2007), Arabian Sea response to monsoon variations, *Paleoceanography*, *22*, PA4217, doi:10.1029/2007PA001467.

1. Introduction

[2] The most studied aspect of the tropical Indian Ocean (IO) is its dynamic response to the seasonally reversing monsoonal forcing [e.g., *Lighthill*, 1969]. Numerous observational and modeling studies over the last few decades have focused not only on the dynamics of the monsoon circulation (see *Schott and McCreary* [2001] for a recent review) but also on the thermodynamics, ecosystem, and biogeochemistry of the IO (see references of *Schott and McCreary* [2001], *McCreary et al.* [1996], *Winguth et al.* [1994], and *Wiggert et al.* [2002]). The role of the IO in monsoon variability has been debated since the early studies of *Shukla and Misra* [1977] and *Weare* [1979] but no consensus has been reached (see *Annamalai and Murtugudde* [2004] for a recent review). Much renewed interest in recent years in the IO has been driven by a purported internal coupled mode called the IO Zonal/Dipole Mode (IOZDM) and its impacts [*Murtugudde and Busalacchi*, 1998; *Murtugudde and Busalacchi*, 1999; *Saji et al.*, 1999; *Webster et al.*, 1999; *Annamalai et al.*, 2005]. The surface warming of the IO in the last few decades has also raised some questions about the response of the IO to anthropogenic activities and its impact on global climate variability [*Levitus et al.*, 2000; *Charles et al.*, 1997; *Hoerling and Kumar*, 2003; *Giannini et al.*, 2003]. Variability of the monsoons themselves span all timescales from intraseasonal to multidecadal and centennial [*Webster et al.*, 1998; *Anderson et al.*, 2002; *Overpeck et al.*, 1996]. While the role of the IO sea surface temperatures (SSTs) in monsoon variability may not be well resolved, the response of the Arabian Sea to monsoonal variability is fairly well understood with enhanced surface cooling during strong monsoons [*Shukla and Misra*, 1977; *Weare*, 1979]. While the meteorologists presumed an increase in evaporative cooling due to strengthened Findlater Jet, oceanographers have often invoked stronger coastal and open-ocean upwelling off the Arabian Peninsula as well as the open ocean evaporative cooling as a means to explain variabilities preserved in the sediment cores and the corals [e.g., *Jung et al.*, 2002; *Altabet et al.*, 2002; *Anderson et al.*, 2002; *Ivanochko et al.*, 2005]. *Vinayachandran* [2004] used satellite surface chlorophyll estimates to compare weak and strong monsoon years to argue that the strength and duration of the southwesterlies are more important for the Arabian Sea cooling rather than the amount of rainfall on the Indian subcontinent. We are not aware of any other studies which have quantified the contribution of coastal or open ocean upwelling vs. the evaporative cooling to the SST changes in the Arabian Sea and how these relative contributions may affect the interpretation of biological proxies and their relation to the strength of the monsoons. The focus of our study is to examine the mixed layer heat budget of the Arabian Sea in a forced ocean general

[1]Earth System Science Interdisciplinary Center and Department of Atmospheric and Oceanic Science, University of Maryland, College Park, Maryland, USA.
[2]Physical Oceanography, Lamont-Doherty Earth Observatory, Columbia University, Palisades, New York, USA.
[3]Department of Marine Sciences, University of Southern Mississippi, Stennis Space Center, Mississippi, USA.

0883-8305/07/2007PA001467

circulation model (OGCM) to provide the dynamical and thermodynamical context to the Arabian Sea response to monsoon variability.

[3] Variability in the strength of the monsoons at centennial and millennial scales has been reported in a number of studies [e.g., *Anderson et al.*, 2002; *Charles et al.*, 1997; *Jung et al.*, 2002; *Gupta et al.*, 2003; *Ivanochko et al.*, 2005]. Whether it is the $\delta^{18}O$ changes from foraminifers or banded corals, the interpretation of cooling has been that strong monsoons drive stronger upwelling and evaporative cooling in the Arabian Sea. The observational and modeling studies of the Arabian Sea heat budget have focused on the seasonal to interannual variability [*Rao and Sivakumar*, 2000; *McCreary et al.*, 1993; *Murtugudde et al.*, 2000] without the paleocontext in mind. Ecosystem and biogeochemical studies have also focused on their response to seasonal and interannual variability of the circulation [*Winguth et al.*, 1994; *Wiggert et al.*, 2002, 2006; *Murtugudde et al.*, 1999].

[4] We revisit the issue of the Arabian Sea response to monsoon variations by contrasting OGCM simulations with composite strong and weak monsoon wind forcing. The impact on surface ecosystem response is examined in a coupled physical-biogeochemical model simulation by contrasting strong and weak monsoon years from an interannual simulation. The main conclusion of the study is that strong monsoons indeed lead to stronger coastal upwelling, lending credibility to the interpretation of paleorecords collected from the coasts or coastal speleothem. The story is however a bit more complicated in the open Arabian Sea since strong monsoons and the strengthened Findlater Jet are associated with negative and positive wind stress curls and thus lead to a deeper thermocline but the stronger winds also lead to deeper mixed layers and entrainment cooling. The net heat flux from the atmosphere into the ocean is then enhanced, indicating a strong oceanic control on the air-sea interactions. Enhanced coastal upwelling and associated nutrient injection into the surface layer result in higher advective fluxes by eddies, jets, and the mean flow into the open ocean. Clearly, the responses of the ecosystem away from the coasts are affected by these fluxes as discussed in the following sections on the heat budget and ecosystem responses. We describe the model and the forcings in section 2 with the main results in section 3. Some concluding thoughts are offered in section 5 with a paleocontext for our model results.

2. Model Description and Forcings

[5] The OGCM used in this study is a reduced gravity, primitive equation, sigma coordinate model and has been described in detail in several prior publications [*Murtugudde et al.*, 1996; *Murtugudde and Busalacchi*, 1999; *Murtugudde et al.*, 2000]. The vertical structure of the model consists of a variable depth oceanic mixed layer [*Chen et al.*, 1994] and a number of sigma layers below. Surface mixed layer is prognostically determined by entrainment-detrainment, shear flow instability, and free convection in the thermocline by combining the physics of the *Kraus and Turner* [1967] mixed layer model with the *Price et al.* [1986] dynamical instability model. The model is capable of ably reproducing the observed dynamics and thermodynamics of the IO including the impact of the Indonesian Throughflow [*Murtugudde et al.*, 1998] at seasonal to interannual and longer timescales. Surface heat fluxes are computed by coupling the OGCM to an advective atmospheric mixed layer (AML) of *Seager et al.* [1995] which has been shown to serve as an excellent tool for computing SSTs without any feedbacks to observations or any restorative fluxes [*Murtugudde et al.*, 1996]. This is crucial for heat budget studies such as this one where the role of the oceanic processes and the thermodynamic response of the lowest layer of the atmosphere to SST changes need to be represented accurately. The model is forced here with the weekly mean scatterometer winds [*Morey et al.*, 2005] along with climatological radiation from Earth Radiation Budget Experiment (ERBE), cloudiness from International Satellite Cloud Climatology Project, and precipitation from CPC Merged Analysis of Precipitation (CMAP) as by *Murtugudde et al.* [1996].

[6] The AML computes air temperatures and humidities for the SST distribution prognosticated by the OGCM which are then used in bulk formulae to compute the latent, sensible, and long wave fluxes given the wind speeds and cloudiness, i.e., quantities that are not directly controlled by SSTs. The most important advantage of this interactive heat flux formulation is that nonlocal effects like the advection of continental air masses onto the ocean are accurately accounted for and such influences are important for the Arabian Sea for both summer and winter monsoon seasons.

[7] The model domain for simulations used here covers 10°S–30°N and 32°E–110°E with a uniform horizontal resolution of ¼ degree and 24 sigma layers in the vertical below the surface mixed layer. Sigma layer thicknesses are ~10 m in the top 200 m increasing to ~300 m near the motionless abyssal layer. River discharges are included as estuarine flow similar to *Han et al.* [2001]. Since the model results for the IO have been reported in the references cited above, we will not present any details other than to mention that the model SSTs are within 1°C of observed SSTs in the whole domain. Since our interest here is to contrast strong and weak monsoon impacts on the IO, the model is perfectly adequate and performs as well as any state of the art OGCM in the IO.

[8] The National Centers for Environmental Prediction (NCEP) reanalyses weekly 10 m winds [*Kalnay et al.*, 1996] are used to identify strong and weak monsoons as the years where mean Somali Jet (zonal winds averaged over 50°E–70°E, 5°N–15°N) for June-August is stronger or weaker than one standard deviation from the mean for 1948–2005. Strong monsoon years according to this criterion are 1955, 1956, 1959, 1961, 1970, 1975, 1983, 1988, and 1994 whereas 1951, 1965, 1966, 1968, 1972, 1974, 1979, 1982, 1986, 1987, and 2002 are identified as weak monsoon years. There is indeed a statistically significant correlation between the Somali Jet defined as above and the all India monsoon rainfall (AIMR) (see Figure 1) even though there are a number of years where the two are out of phase. This is not unexpected since external forcings such as El Niño–Southern Oscillation (ENSO) teleconnec-

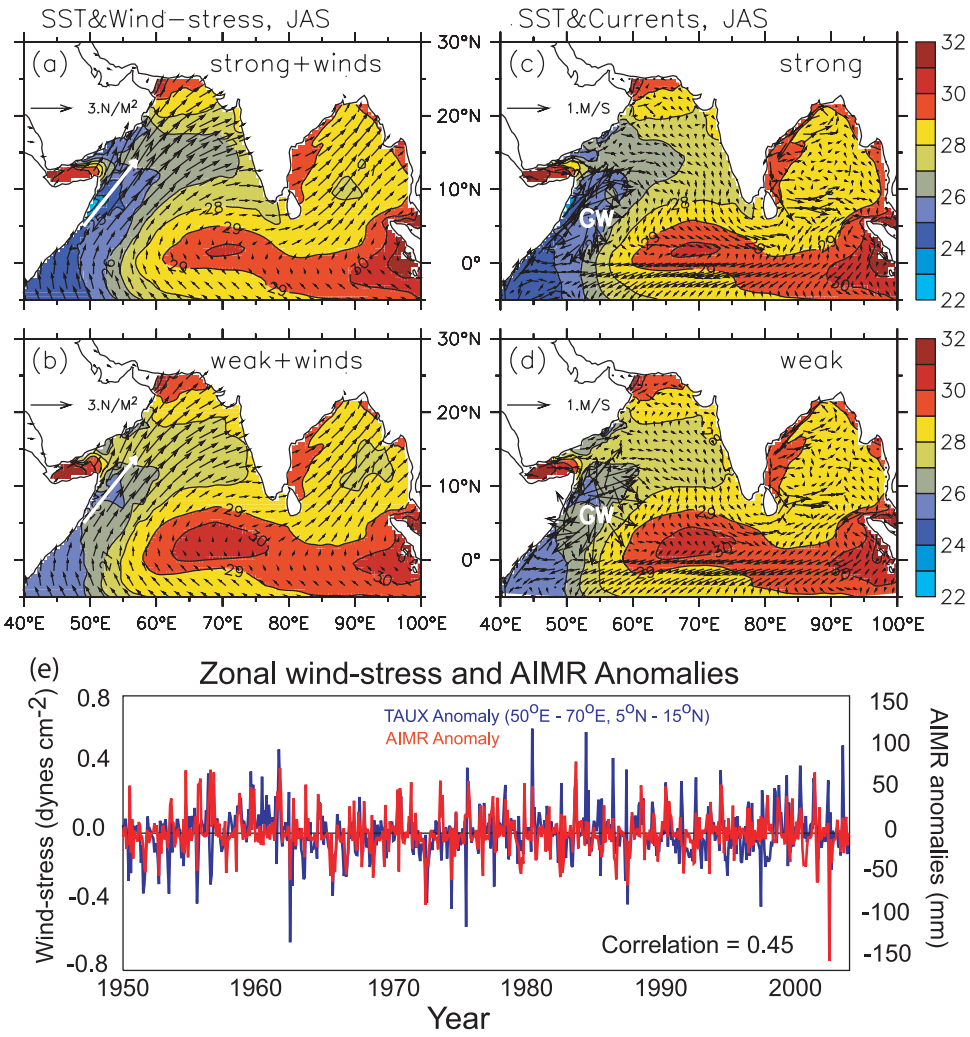

Figure 1. (a–d) Mean model SSTs for July–September for the strong winds plus wind speeds and weak winds plus wind speeds (see text for explanation) with corresponding winds overlaid (Figures 1a and 1b); mean SSTs for July September for strong and weak winds with currents overlaid (Figures 1c and 1d). The white arrows represent the Somali Jet, which is the surface expression of the Findlater Jet and "GW" identifies the Great Whirl. (e) Correlation between the Somali Jet defined as the zonal wind stress averaged over the Arabian Sea region indicated and the All India Monsoon Rainfall. The zonal wind stresses are computed from the NCEP reanalysis 10 m winds with a constant drag coefficient of 1×10^{-3}. The correlation coefficient of 0.45 is statistically significant at the 95% level.

tions involve both atmospheric and oceanic bridges which affect the Somali Jet and the AIMR differently and on different timescales [see, e.g., *Alexander et al.*, 2002; *Annamalai and Murtugudde*, 2004]. We simply composite the calendar years identified as strong and weak monsoons respectively to generate weekly climatology of the winds to simulate the IO responses. Note that there is a high correlation between the strength of Findlater and Somali jets to the Indian monsoon [*Findlater*, 1969], although a few of the years from the rainfall criterion for strong and weak monsoons do not match the wind criterion used here. However, paleorecords are typically interpreted as representing monsoon variability in terms of strong or weak wind forcing over the Arabian Sea and our methodology to create the forcing is consistent with that interpretation. It should also be noted that this approach of compositing strong and weak monsoons from the modern climate is quite simplistic and idealized since nearly all paleostudies referred to here are associated with significantly different global climate in terms of ice cover, SSTs, and winds. However, our main conclusions are not fundamentally affected by this simplification.

[9] The OGCM has been coupled to a biogeochemical model which has been described by *Christian et al.* [2002], *Wiggert et al.* [2006], and *Wang et al.* [2006]. The ecosystem model consists of two size classes of phytoplankton, zooplankton, and detritus, respectively with simultaneous iron and nitrogen limitations. Model simulations of the nitrate distributions, surface chlorophyll, primary and export productions compare favorably with available observations

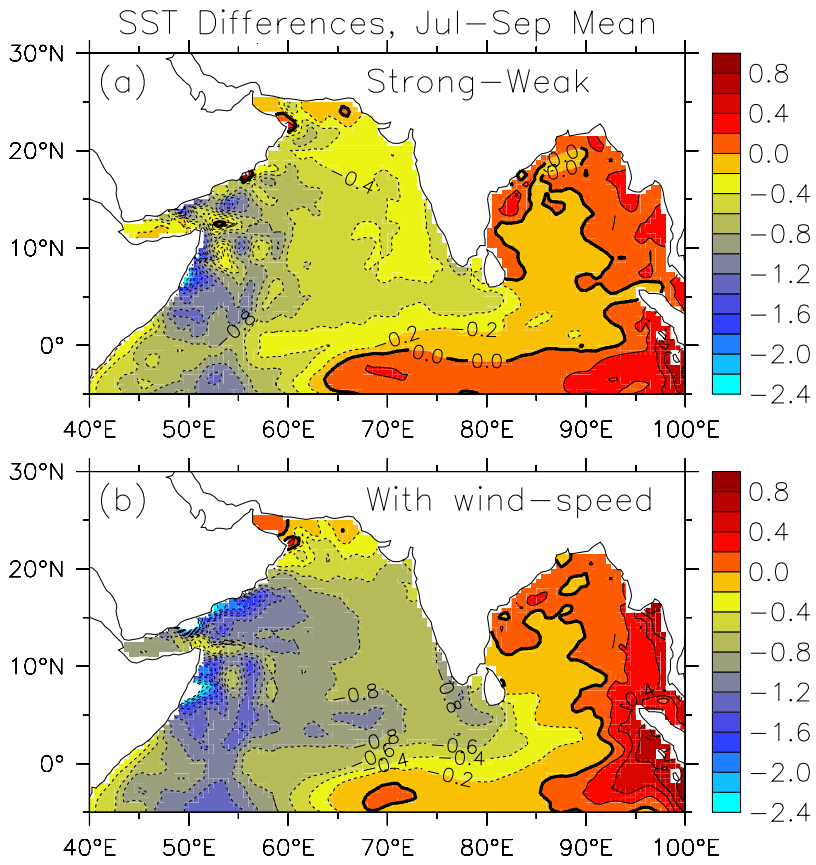

Figure 2. July–September mean SST differences (a) between strong and weak monsoon wind stress forcing and (b) for strong and weak monsoon wind stress plus wind speed forcing. The latter also account for the impact of wind speeds on evaporative cooling. Contour interval is 0.2°C.

at seasonal to interannual timescales. An interannual simulation of the coupled biogeochemical OGCM (BOGCM) is performed for 1948–2003 with the forcings as described by *Wang et al.* [2006]. We contrast surface chlorophyll, primary, and export production for the strong and weak monsoon years as identified above.

3. Model Response to Monsoon Variability

[10] The OGCM is spun up with weekly climatologies of scatterometer winds for 25 years to produce the initial state for the strong and weak composite monsoon simulations. The strong and weak monsoon forcings are imposed for additional 10 years starting from the same initial conditions and the means of the last 5 years are used to analyze the impact of monsoon variability on the Arabian Sea. To separate the dynamical effects of monsoonal wind changes from the thermodynamical effects, model simulations are carried out with wind stress forcing only with the wind speeds in the latent heat flux calculations held to the climatological values (winds-only simulation). Additional simulations are carried out with strong and weak monsoon wind speeds in the latent heat flux calculations in addition to the wind stress forcing (winds plus wind speed forcing). This allows us to quantify additional ocean responses due to any evaporative changes associated with the wind speed changes [also see *Murtugudde and Busalacchi*, 1999]. We contrast the strong and weak monsoon forced simulations in both cases to quantify the impact of wind-driven upwelling changes and upwelling plus the evaporative cooling impacts. Since our goal is to understand the role of monsoon variability in sequestering the biogenic signals in paleorecords and since the monsoonal changes we are after are of decadal and longer timescales, we contrast only the summer months (July–September) and neglect the impact of winter monsoon changes. Note that the Bay of Bengal also responds to wind changes associated with monsoon variability but they are not discussed here since our focus is on the Arabian Sea. The initial state for the interannual simulation of the BOGCM is generated by spinning up the model for 25 years with weekly climatologies of the NCEP Reanalyses winds following which, the interannual weekly means are used to simulate the 1948–2003 period to analyze the strong and weak monsoon years identified in the previous section.

3.1. Surface Response

[11] The July–September mean differences in SSTs for winds-only and winds plus wind speed forcing are shown in Figure 2. The dynamical response to winds alone produces SST cooling of ~0.6°C off Somalia and the Arabian Peninsula. Maximum cooling along the coast is a clear

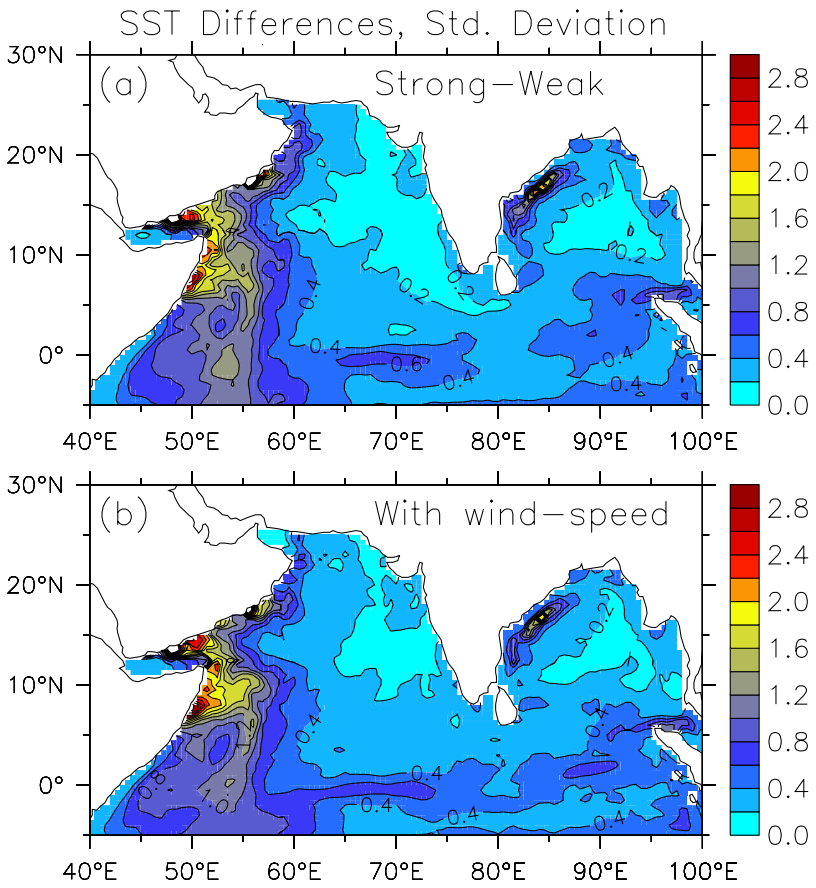

Figure 3. Standard deviation of the July–September SST differences (a) for the strong and weak wind stress forcing and (b) for strong and weak wind stress plus wind speed forcing. Contour interval is 0.2°C.

indication that upwelling is indeed stronger for strong monsoons compared to years with weak monsoons. The striking result however is that even the coastal cooling is more than 80% stronger and the open ocean cooling is more than 50% stronger when the enhanced entrainment associated with wind speed changes accompanying the stronger monsoons is included (note that entrainment is always associated with the deepening of the mixed layer driven by surface turbulent kinetic energy [see *Chen et al.*, 1994]). Enhanced cooling extends all the way into the lower Bay of Bengal. The standard deviations of the SST differences shown in Figure 3 make it obvious that the variability of coastal upwelling is greatly enhanced off Somalia and at the mouth of Gulf of Aden to the Omani coast with a signature also off the east coast of India. This immediately corroborates the interpretation of biogenic paleorecords that enhanced biological activities in the coastal regions must be related to the strengthening of the summer monsoons [e.g., *Altabet et al.*, 2002; *Ivanochko et al.*, 2005]. This is not as obvious for the cooling in the Arabian Sea and the extension into the Bay of Bengal. The regions of large standard deviation of SST differences between strong and weak monsoons can be used to enhance paleodata gathering in the absence of full-blown optimization of observations [see, e.g., *Ballabrera-Poy et al.*, 2007] since they correspond to larger variability in the oceanic response to strong and weak monsoons.

[12] The easiest check on wind-driven upwelling is of course the wind stress curl which is shown for strong and weak monsoons in Figure 4. The alongshore winds clearly enhance the upwelling whereas a stronger Somali Jet is accompanied not only by stronger wind speeds but also by larger negative wind stress curl which drives downward Ekman pumping and a deeper thermocline. Deeper mixed layers are also seen in Figure 5 indicating that the stronger wind speeds and the weaker stratification associated with the deepening of the thermocline lead to mixed layer entrainment. Note that the mixed layer shallows to the northwest in the positive wind stress curl region due to Ekman pumping and to the southwest where wind stress curl is positive or near zero. All the summer difference fields highlight the circulation features such as the Great Whirl [*Schott and McCreary*, 2001] which is the main recirculation feature in the coastal region associated with the instability of the Somali Current as it crosses the equator. The anticyclonic Great Whirl is a convergent feature with deeper mixed layer and thermocline in the center and cold, upwelled waters being advected around the rim during strong monsoon epochs. More importantly, the deepening of the mixed layer extends into the open ocean and as expected wind speed effects and enhanced turbulent

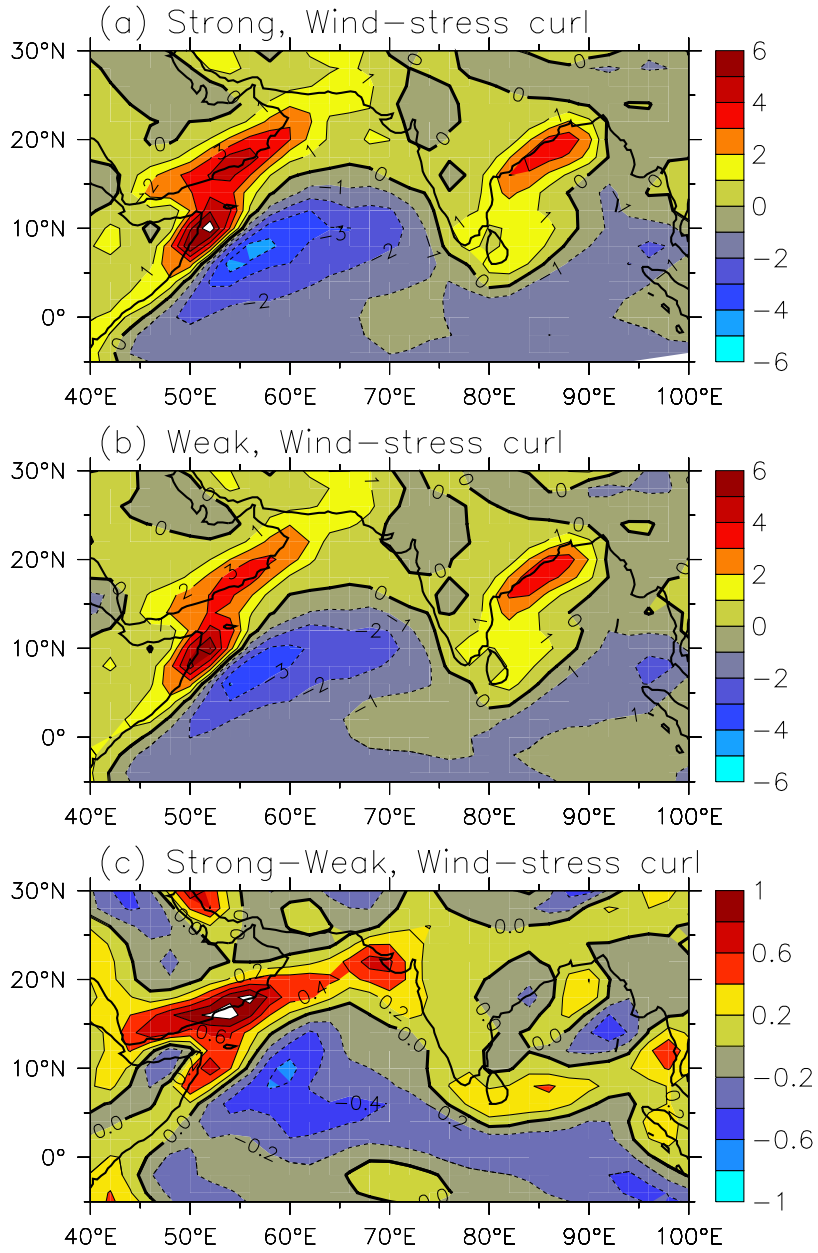

Figure 4. Wind stress curl ($\times 10^{-6}$ N m^{-3}) for (a) strong and (b) weak monsoons and (c) their difference averaged for June–August period, showing enhanced Ekman pumping at the coast and Ekman downwelling in the open ocean. Positive (negative) values indicate Ekman divergence (convergence). White regions in Figure 4a are curls greater than 6×10^{-6} N m^{-3}.

kinetic energy exacerbates the weaker stratification and deepening of the thermocline and the mixed layer (also see Figure 6). In the regions where wind stress curl is not accompanied by stronger wind speeds, Ekman pumping typically results in convergence and surface warming whereas the deepening of the mixed layer in the central Arabian Sea is characterized by convergence of colder waters in addition to enhanced entrainment. The warming due to the convergence is seen deeper in the thermocline below ~100 m (see Figure 7). The Bay of Bengal is affected by upwelling off Sri Lanka and the intrusion of this water into the mouth of the bay [see *Murtugudde et al.*, 1999], whereas the head of the bay is more akin to the Arabian Sea with deeper mixed layer and thermocline.

3.2. Subsurface Response

[13] Larger negative wind stress curls in the southern Arabian Sea during strong monsoons (Figure 3) which lead to a deeper thermocline as shown in Figure 5, should also result in increased southward Sverdrup transport. The compensating return flow occurs through stronger northward transports in the western boundary current along

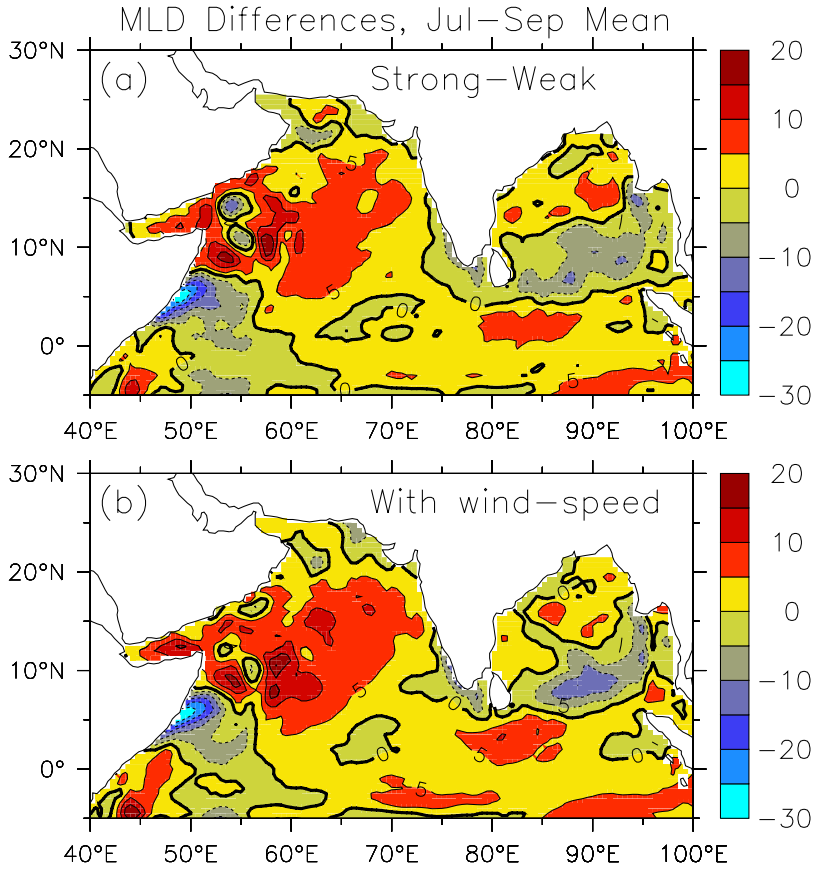

Figure 5. Differences in mixed layer depths (MLD, m) for (a) strong and weak wind forcing only and (b) winds plus wind speed forcing averaged for July–September period.

Somalia (not shown). A shallower thermocline is seen all along the coasts including the west coast of India (Figure 6). One would expect stronger upwelling to reduce mixed layer depths but the stronger winds and surface cooling also generate turbulent kinetic energy and entrainment which tend to deepen the mixed layer. The increase in upwelling thus tends to increase colder waters and nutrients below the mixed layer and the surface entrainment cools the surface and drives surface biological production.

[14] For assessing the impact of monsoon variability on biological production, we must ensure that the surface cooling is indeed associated with deeper coastal upwelling and not simply related to the cooling due to entrainment. That this is indeed the case is seen in Figure 7 as cooler temperatures extending well into the thermocline (and the nutricline), especially near the coasts. For both wind forcing only and wind plus wind speed forcing simulations, coastal upwelling draws waters from up to 200 m depth when monsoons are stronger, advecting it offshore to the east into the Arabian Sea. Wind speed effects not only enhance surface cooling in the open ocean but also deepen the thermocline further, which are reflected by warmer temperatures in the right panel of Figure 7. These processes have consequences for primary production in the Arabian Sea and thus will impact the biogenic signals in the coastal and offshore paleorecords. The species composition will also be affected by a stronger coastal upwelling while the open ocean cooling does not necessarily enhance surface production unless the deeper mixed layers and the thermocline are associated with increased nutrient supply [*Wiggert et al.*, 2006]. The examination of the heat budgets indicate that stronger Somali Current is associated with enhanced advection into the open ocean which also transports nutrients.

3.3. Heat Budget

[15] Mixed layer heat budgets provide a quantitative measure of the contributions from surface forcings and vertical vs. horizontal processes to the SST variability. Advection and entrainment associated with the SST cooling are also associated with nutrient transports and are strong indicators of biogenic production. This quantification is essential for guiding both the interpretation of surface and subsurface variability proxies such as the $\delta^{18}O$ of corals and thermocline dwellers [e.g., *Charles et al.*, 1997; *Jung et al.*, 2002]. The SST equation is the same as the one from *Chen et al.* [1994] and *Jochum and Murtugudde* [2005]. In the prognostic equation for SST,

$$T_t = Q_{net} + Q_D + Q_H + Q_w,$$

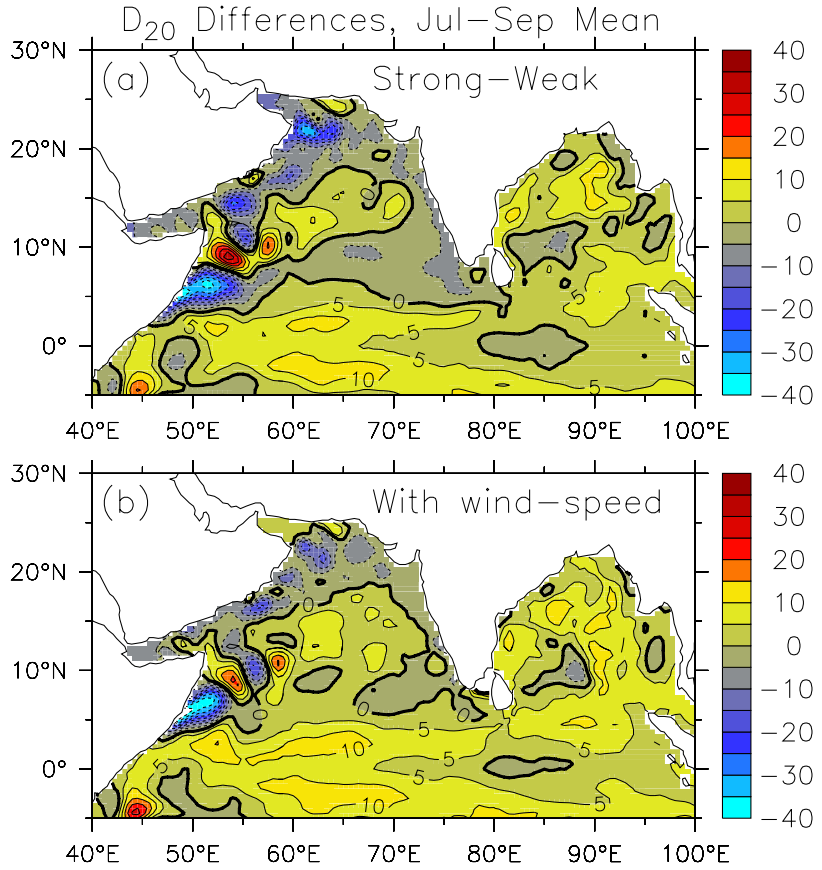

Figure 6. Differences in the depths of 20°C isotherms (D_{20}, m) for (a) strong and weak wind forcing only and (b) winds plus wind speed forcing averaged for July–September period.

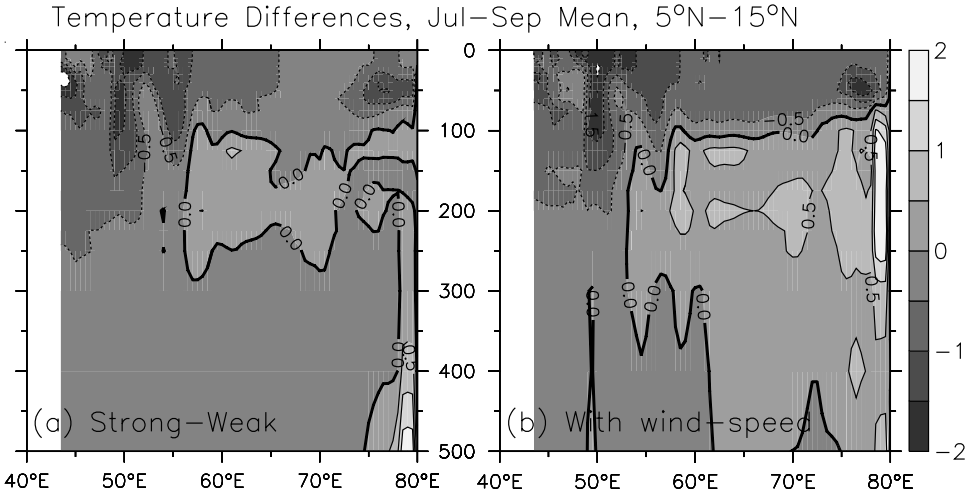

Figure 7. Temperature differences (°C) averaged over 5°N–15°N in the Arabian Sea (a) for wind forcing and (b) for wind plus wind speed forcing averaged for July–September period. Coastal upwelling extends deeper for strong monsoons and surface cooling is stronger with wind speed forcing included.

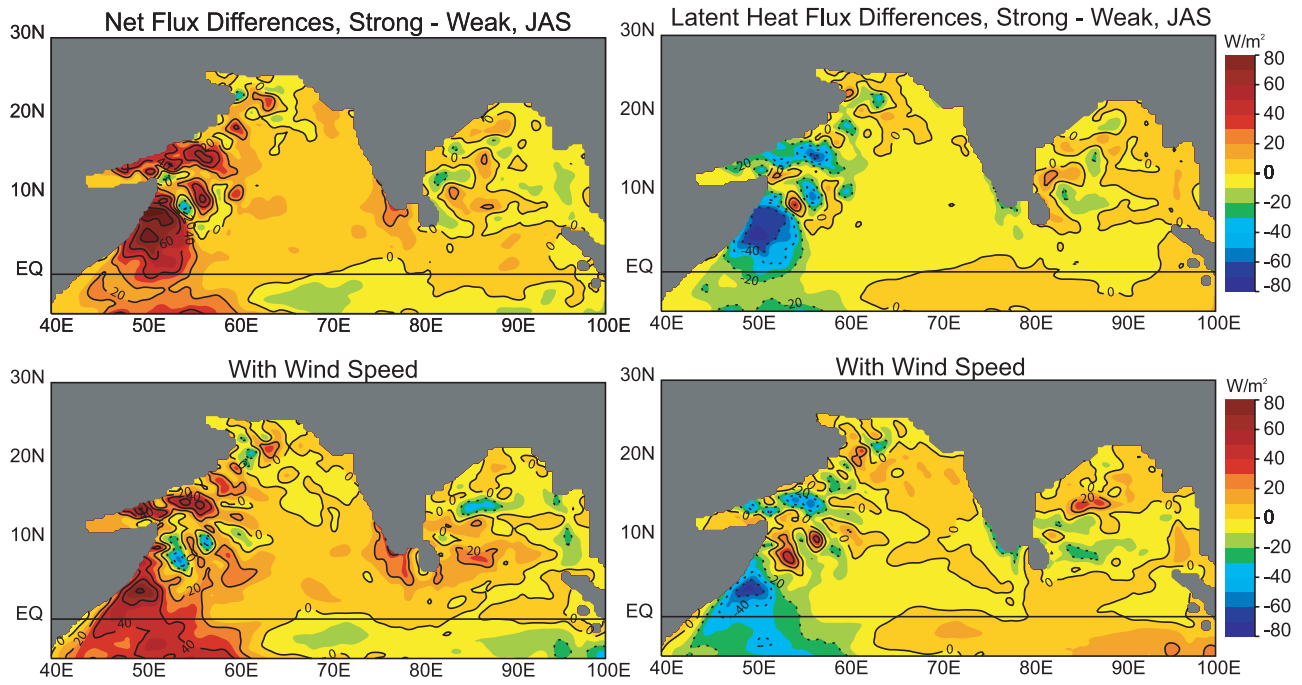

Figure 8a. Heat budget terms (W m^{-2}) for model simulations with wind forcing only and winds plus wind speed forcing; differences averaged over July–September for (left) net heat flux and (right) latent heat loss. Net heat flux is positive into the ocean and latent heat loss is positive out of the ocean.

[16] T_t is the rate of change of SST; Q_{net}, the net surface heat flux divided by the mixed layer depth, Q_D is the sum of vertical and horizontal mixing, Q_H is the horizontal advection (zonal plus meridional) and Q_w is the vertical advection. As stated in section 2, the mixed layer deepening and the required entrainment are computed by balancing the surface turbulent kinetic energy against the stratification below the mixed layer [*Chen et al.*, 1994]. The net heat flux is computed as

$$Q_{net} = Q_S - Q_{LH} - Q_{SH} - Q_{LW} - Q_{pen},$$

where Q_S, Q_{LH}, Q_{SH}, Q_{LW}, and Q_{pen} are the solar radiation, latent heat loss, sensible heat flux, long wave radiation, and penetrative heat loss, respectively. Penetrative radiation is computed as by *Murtugudde et al.* [2002] and is not an important player in this analysis and hence not discussed further here. Our convention for the net heat flux is positive when it is downward (heating the ocean) whereas the latent heat loss is positive upward (cooling the ocean).

[17] Major contributors to the heat budget are the net surface heat flux with latent heat flux being the largest component, zonal and meridional advections, and entrainment of subsurface waters into the surface mixed layer. We present the July–September mean differences in the heat budget terms corresponding to the SST differences in Figure 2 and we also present the differences for simulations with wind forcing only and wind plus wind speed forcing. The net heat flux over the Arabian Sea during much of the spring intermonsoons (March–May) and early summer monsoons is downward from the atmosphere into the ocean but the peak heating is reached prior to the onset of the monsoons [*Rao and Sivakumar*, 2000; *Murtugudde and Busalacchi*, 1999]. Once the Somali Jet is well formed, the atmospheric heating begins to drop and the Arabian Sea in fact loses heat to the atmosphere during the peak summer monsoon months of June–July August. The ocean is heated again during the boreal fall months but the cold and dry air masses off the continents cool the ocean during the boreal winter months. Annual mean heat fluxes are largely from the atmosphere into the ocean and are of order ~20 W m^{-2}.

[18] Annual mean heat flux differences for strong and weak monsoons with and without wind speed forcing are positive over much of the Arabian Sea in Figure 8a corresponding to enhanced heat uptake by the ocean or reduced heat loss form the ocean which is expected by the surface cooling seen in Figure 2. Maximum differences, expectedly in the coastal upwelling regions, of ~40 W m^{-2} are quite significant and mostly damp the monsoon-related SST cooling. Reduced latent heat losses of similar magnitudes point to the control ocean dynamics on surface cooling, which in turn lowers the evaporative cooling along the coasts despite stronger wind speeds. Enhanced evaporative cooling by including the wind speed effects is clearly minimal which is surprising and noteworthy, especially for interpreting paleoproxies. This is a clear indication that the ocean dynamics largely control SST cooling along the coast during strong monsoons and the atmosphere responds to SSTs by damping the anomalies. Note that in a fully coupled climate system such mesoscale SST cooling and coastal upwelling fronts are also associated with wind responses [*Vecchi et al.*, 2004] which we are only partially

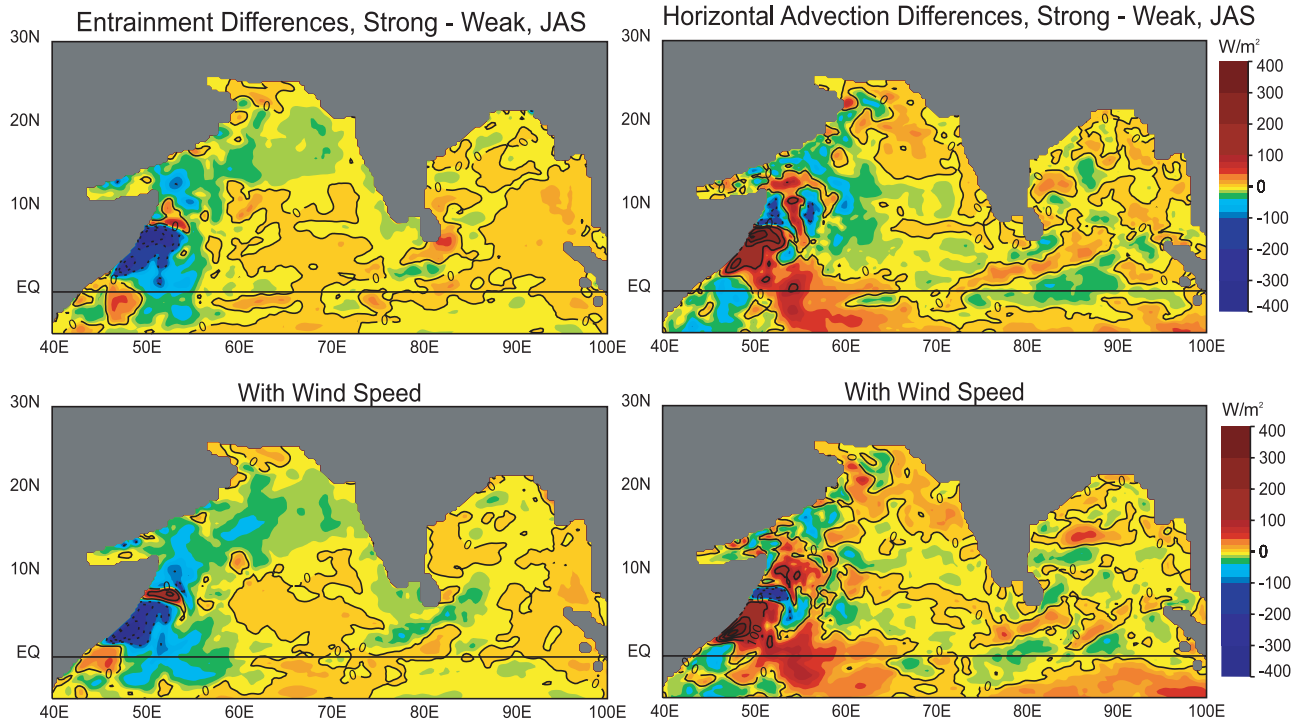

Figure 8b. Same as Figure 8a but for entrainment and advection terms of the SST heat budget (W m^{-2}). Negative differences in entrainment flux correspond to enhanced surface cooling. Regions with positive advection differences correspond to local warming by advective fluxes.

accounting for by employing observed winds associated with strong and weak monsoons.

[19] The strongest coolings in the coastal upwelling regions are a combination of enhanced entrainment cooling (negative differences correspond to larger entrainment flux into the mixed layer) and strong horizontal advection of the upwelled waters entrained into the mixed layer (Figure 8b). Much of the Arabian Sea SST variability can be explained as a one-dimensional balance between surface heating and downward mixing of heat by mixed layer entrainment processes [e.g., *Rao and Sivakumar*, 2000; *Murtugudde and Busalacchi*, 1999; *Murtugudde et al.*, 2000]. The July–September differences in horizontal heat advection (Figure 8b; regions with positive differences are locally heated by advection and regions with negative differences are being cooled by the advective contributions) show mesoscale features in the coastal upwelling region with large cross-gradient advection as by *Jochum and Murtugudde* [2005]. However, the horizontal advection makes a net contribution to the open ocean and this could be an important source of nutrients for surface primary production (see Figure 9) [see also *Wiggert et al.*, 2006]. The central Arabian Sea is cooled by the horizontal advection, but the southern and northern Arabian Sea are warmed in the summer months due to enhanced convergence into the core of the Somali Jet region. The largest contribution to the cooling in the coastal and open ocean region is clearly from the mixed layer deepening and the entrainment of cold waters, while convergence of cooler waters making a significant contribution in the open ocean. The upwelling in the coastal regions supplies cold waters to the bottom of the mixed layer and the mixed layer entrainment injects this water into the surface cooling the SSTs. Wind speed forcing also contributes to enhanced surface turbulent kinetic energy and deeper mixed layers (Figure 5).

[20] To make the mixed layer heat budget clearer in the open ocean, Figure 9 shows the annual cycle of the differences in the main SST equation terms averaged over 50°E–70°E, 5°N–15°N. Ocean dynamic control on SSTs in the Arabian Sea is evident as a net increase in downward heat flux during most of the year in response to SST cooling. Strong entrainment cooling occurs mostly during the summer months and including the wind speed effects shows that evaporative cooling makes a small contribution to reducing the differences in entrainment cooling during July–August. Horizontal advection is a predominantly cooling term during the summer months but the mesoscale variability and the cross-frontal advection terms make a net contribution to the open ocean SST variability as seen by the large variability in the boreal summer months.

3.4. Observational Evidence for Arabian Sea Response to Monsoon Variations

[21] Model results presented above are intuitive as far as the cooling of the Arabian Sea in response to strong monsoons is concerned. However, the ocean dynamics appear to be in complete control of the surface cooling with even the latent heat loss being reduced in response to the surface cooling. Latent heat loss is reduced despite the significant increase in wind speeds during strong monsoons.

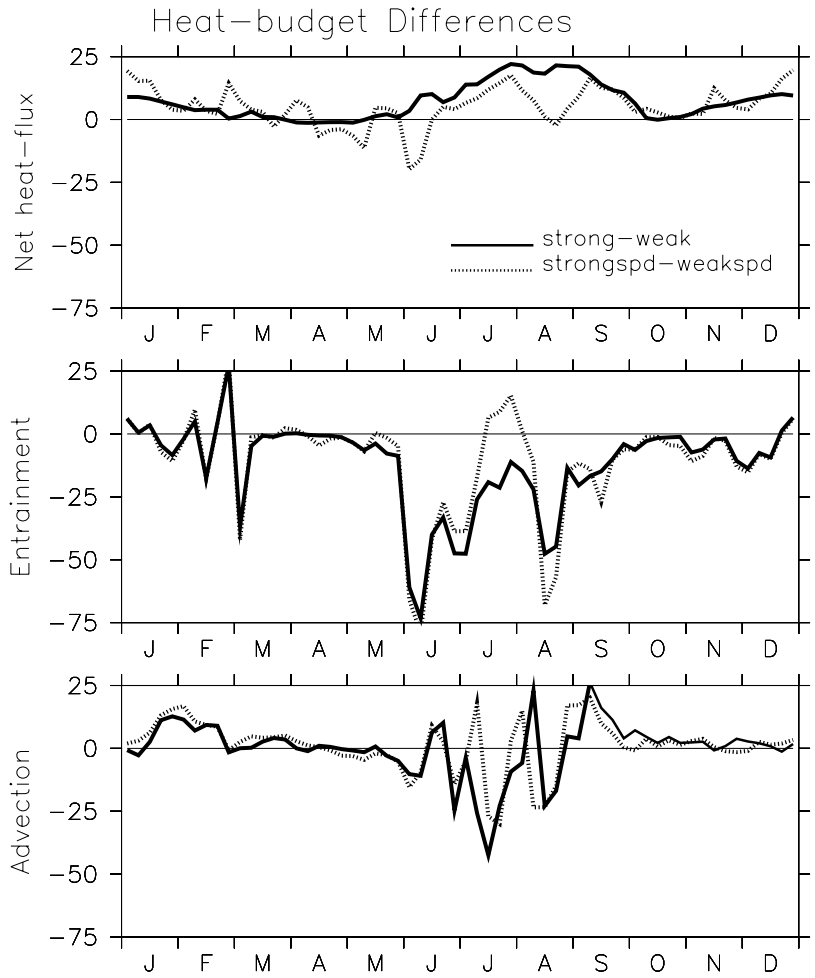

Figure 9. Heat budget terms for the mixed layer averaged over the Arabian Sea (5°N–15°N, 50°E–70°E): (top) net heat flux, (middle) entrainment flux, and (bottom) the horizontal advective fluxes. Net heat flux into the ocean is larger for strong monsoons in response to SST cooling, and the cooling is accomplished by increased mixed layer entrainment and advective fluxes.

This requires that we produce some evidence for similar behavior in the real world. We offer corroborative evidence from two SST products [*da Silva et al.*, 1994; *Reynolds and Smith*, 1994] and from two latent heat flux products [*da Silva et al.*, 1994; *Kalnay et al.*, 1996]. Figure 10 shows the July–September differences for strong and weak monsoon years as defined in section 2 for SSTs and latent heat fluxes from these observational and reanalysis products. Note that the Comprehensive Ocean-Atmosphere Data Set (COADS) product by *da Silva et al.* [1994] is ship based and the fluxes are computed using a bulk formula. The SSTs of *Reynolds and Smith* [1994] are based on buoys and satellites and the NCEP reanalyses product [*Kalnay et al.*, 1996] is a data assimilated model product and is affected by its own biases especially in data-sparse regions such as the Indian Ocean.

[22] It is thus remarkable that despite these disparate observational estimates, the differences in SSTs and latent heat fluxes are in remarkable agreement with the model results; SSTs during the summer months are indeed colder over the Arabian Sea for stronger monsoons. Also, despite the enhanced wind speeds during stronger monsoons, the latent heat losses from the ocean surface do not show expected increases. This serves as clear and convincing evidence that the surface cooling during strengthened monsoon regimes is mostly controlled by enhanced upwelling off the Somali coast and deepening of the mixed layer due to entrainment of subsurface cold waters driven by the higher surface turbulent kinetic energy. The downward Ekman pumping associated with the negative wind stress curls during stronger monsoons is also accompanied by entrainment cooling. Even though the atmospheric response is to damp the SST cooling by increasing net downward heat flux, this flux acts on a deeper mixed layer and thus is less efficient in alleviating the cooling of SSTs by the ocean dynamics.

3.5. Ecosystem Response

[23] We investigate the ecosystem response to monsoon variability in an interannual simulation for the period 1948–

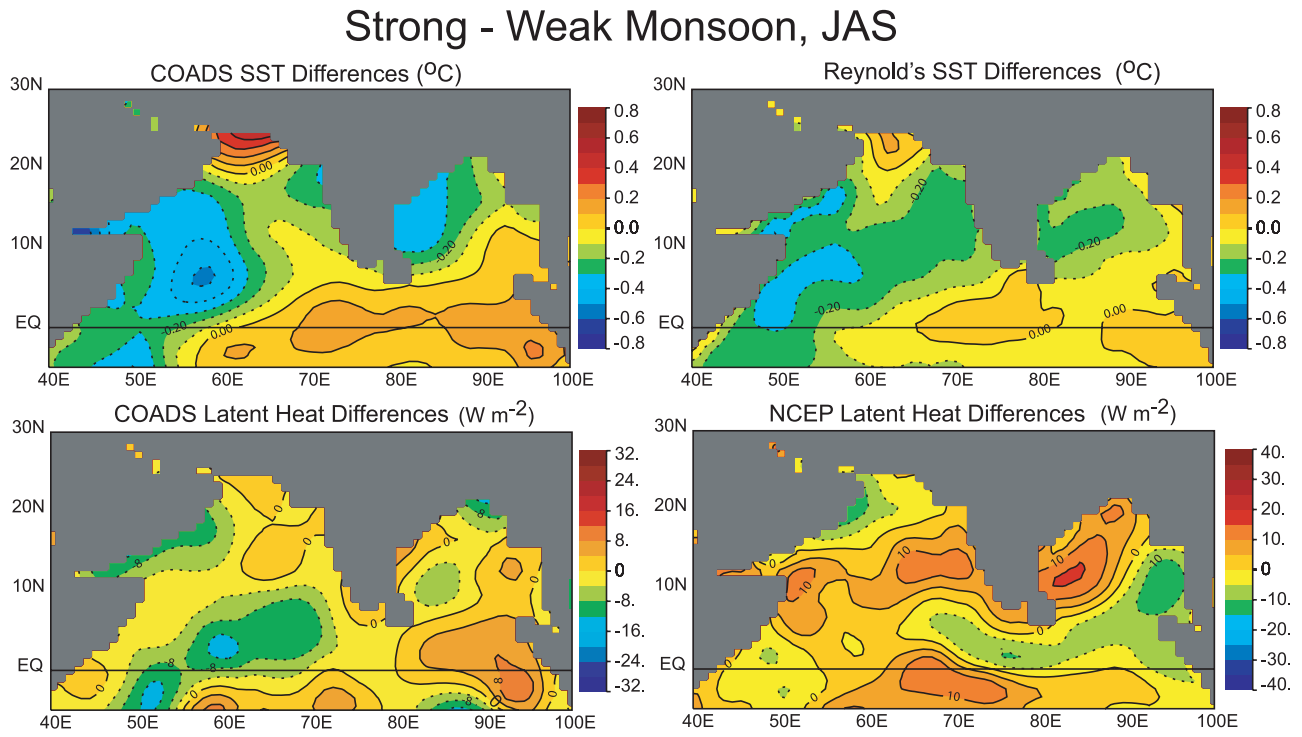

Figure 10. July–August–September mean differences in SSTs and latent heat loses for strong and weak monsoons from (top left) COADS and (top right) *Reynolds and Smith* [1994] SSTs and (bottom left) COADS and (bottom right) NCEP reanalyses latent heat loses (latent heat loss is positive out of the ocean).

2003. As discussed in section 2, the BOGCM is forced with weekly mean NCEP reanalyses winds with the wind speeds computed from the wind stresses and precipitation from CMAP. Thus the wind stresses, precipitation, latent and sensible heat fluxes contain interannual variability whereas the solar radiation and cloudiness are climatologies due to a lack of reliable long time series from observations. The ability of the model to capture much of the observed interannual variability have been discussed by *Murtugudde and Busalacchi* [1999] and *Murtugudde et al.* [2000]. The differences are shown for the strong-weak monsoon years as identified in section 2.

[24] Surface response to strengthened monsoons (Figure 11) clearly consists of enhanced cooling, especially in the coastal regions. It is comforting that the composite strong and weak monsoon forcings produce similar surface cooling albeit the separate core of cooler SSTs in the interannual simulation. Biological response shown in Figure 12 is quite consistent with what is expected, namely, elevated chlorophyll especially near the coast and in the Gulf of Aden. Note also that the Arabian Sea experiences two peaks in surface production, during boreal winter and summer months, but our focus here is still driven by the paleostudies and we thus constrain ourselves to the boreal summer differences. The Great Whirl has a signature as reduced chlorophyll in the convergent interior and enhanced surface chlorophyll in the entrainment ring at the outer edges. Primary production depends not only on the phytoplankton response to monsoonal forcing but also on the growth rates for the small and large phytoplankton and on the depth of the mixed layer over which production is integrated [see *Wang et al.*, 2006]. Thus the pattern of primary production increase is spread over the open ocean and not coincident with the coastal upwelling band of elevated chlorophyll. Over the centennial and longer timescales we are interested in, these signatures will likely be homogenized over the regions where sediments are typically drilled.

[25] For interpreting biogenic paleoproxies, we are more interested in the export production since it is this organic carbon that escapes the upper ocean recycling and leaves a signature that is sequestered in marine sediments. Figure 13 shows the mixed layer differences in export production and longitude-depth distributions integrated over the 5°N–15°N latitude band (the sloping coastline leads to the far west being determined by the Gulf of Aden where the export is locally reduced). It is evident that much of the coastal upwelling region and the Arabian Sea experience enhanced export production and thus the biological signatures in the paleoproxies must show enhanced production for stronger monsoons. It should also be noted that while the focus here has been on the summer monsoons and their impact on the ecosystem response, winter monsoons are also associated with elevated production with the classic Sverdrup mechanism in play [*Wiggert et al.*, 2002]. According to the Sverdrup mechanism, maximum deepening of the mixed

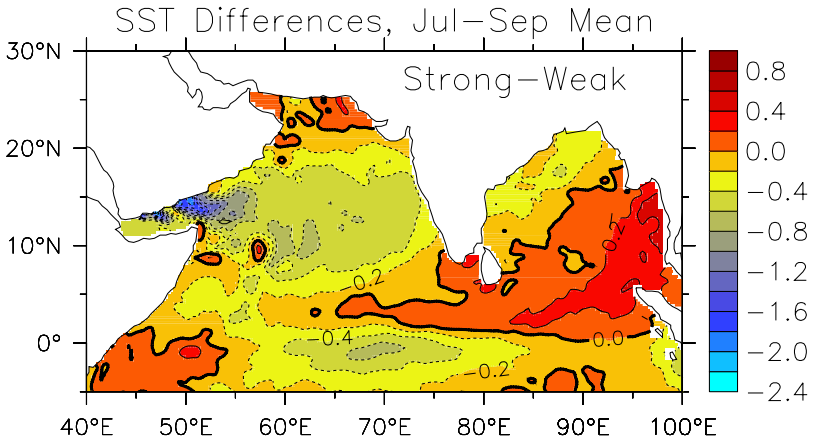

Figure 11. SST differences for July–September for strong and weak monsoon years from an interannual simulation for the period 1948–2003. See text for years corresponding to strong and weak monsoons.

layer due to nighttime cooling is determined by the mean thermocline position. During the boreal winter months, the mean thermocline depth is determined by the large-scale wind stress curl while the nutrient injection into the euphotic zone and the surface production are determined by the diurnal cycle of the mixed layer acting on this thermocline depth. Further studies are needed to quantify the role of the winter monsoons on the Arabian Sea biogenic signatures.

4. Discussion and Concluding Remarks

[26] An OGCM has been employed to quantify the role of oceanic processes in sequestering biogenic signals in the

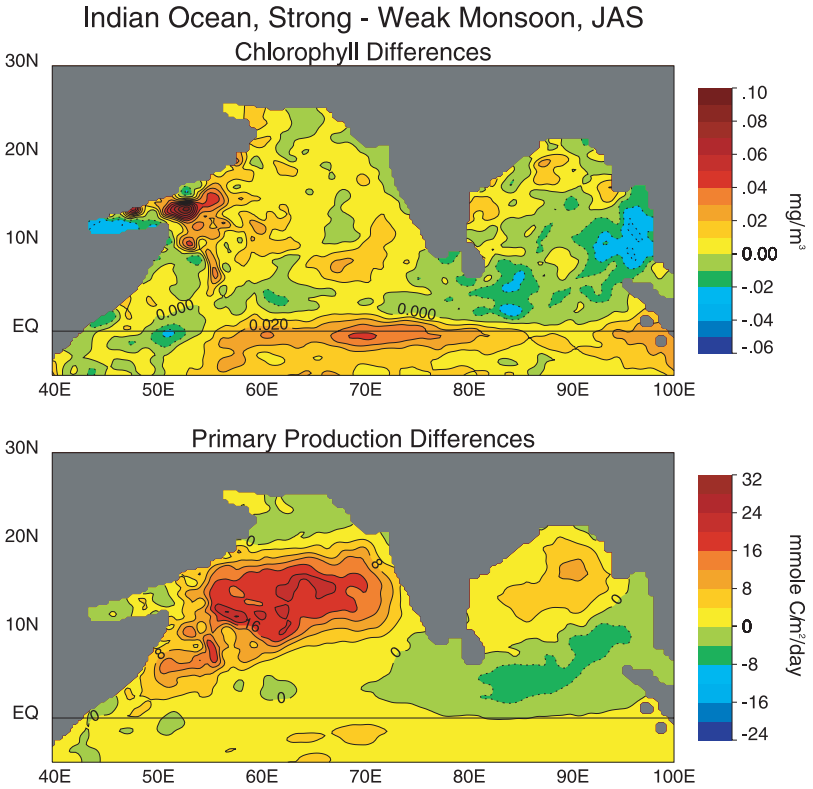

Figure 12. July–September differences in surface chlorophyll and mixed-layer integrated primary production for strong and weak monsoons during 1948–2003. These are computed from an interannual run as opposed to the composite forcings used in the physical simulations.

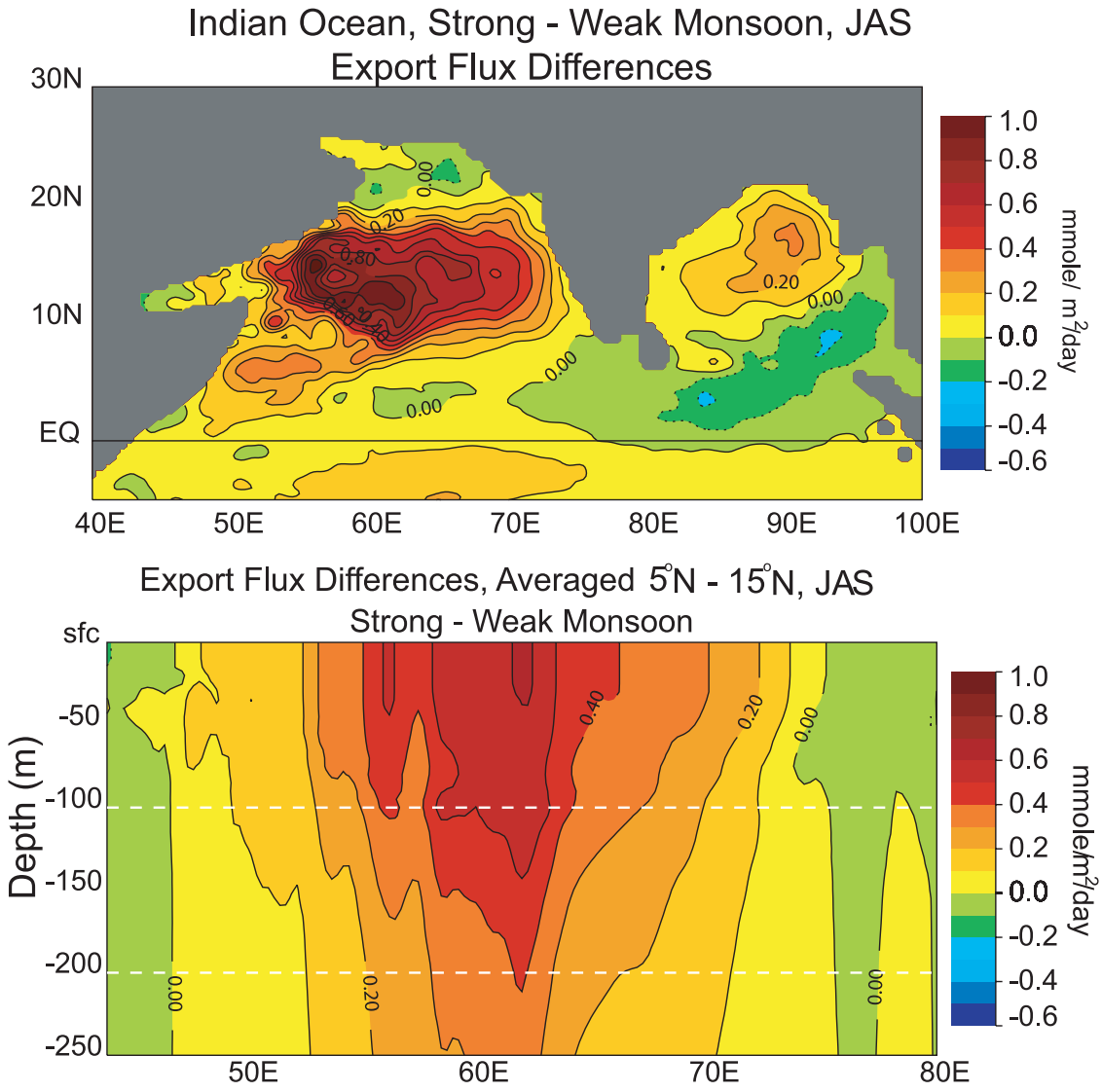

Figure 13. Differences in simulated export fluxes for (top) the mixed layer and (bottom) longitude-depth distribution averaged over 5°N–15°N.

paleoproxies of monsoon variability in the Arabian Sea. A simple methodology is used to generate composite strong and weak monsoon winds for the tropical Indian Ocean by identifying years with stronger (weaker) than one standard deviation of the weekly mean of 10 m zonal winds from NCEP reanalyses averaged over the Arabian Sea (5°N–15°N, 50°E–70°E). Two simulations are carried out by imposing the strong and weak composite monsoons on an OGCM configured for the tropical Indian Ocean and coupled to an atmospheric mixed layer model that has been spun up for 25 years with weekly mean climatological winds. The correlation between the intensity of the Somali Jet and summer monsoon rainfall over India is statistically significant although the explained variance is only ~25% (see Figure 1). An interannual simulation of the same OGCM coupled to an ecosystem model is carried out for 1948–2003 to contrast strong and weak monsoon years in terms of their ecosystem responses.

4.1. Model Results in a Paleocontext

[27] Here we examine the interpretations of paleoclimate proxies in the light of the current model results. *Schulz et al.* [1998] examined cores in the northeastern Arabian Sea (at about 23°N and 65° to 67°E) that record total organic carbon (TOC) and the oxygen isotope ratio of near-surface-dwelling foraminifera. This location has no clear upwelling signal and changes in TOC are interpreted as being remotely caused by changes in upwelling off Oman and advection of nutrient-rich waters northeastward to the core site. According to this interpretation, the record shows strong upwelling off Oman during glacial interstadials and weak upwelling during stadials. In the model results presented here, the sites are generally ones in which produc-

tivity increases during strong monsoons. Hence the model results support a strong (weak) monsoon during interstadial (stadial) link. Consistently, the isotope records from the cores indicate warm upper ocean temperatures during interstadials although the model shows only a weak impact of monsoon variability on SSTs at this site (Figure 2). To be more specific, paleointerpretations invoke either a local increase in productivity driven by increased upwelling due to stronger monsoons or the modification of water properties at intermediate depths to better preserve the biogenic signatures in the sediments. Model results indicate that enhanced upwelling is not valid away from the coastal locations and thus better preservation of biogenic signals due to intermediate water property changes (such as denitrification) is a more likely scenario.

[28] Both *Altabet et al.* [2002] and *Ivanochko et al.* [2005] examined high accumulation sediment records of denitrification (which results from use of nitrate as the oxidant in bacterial breakdown of organic matter in waters where the oxygen concentration is low) in cores off Oman and Somalia, respectively. Both cores resolve millennial climate events during the last glacial and, by comparison with the Greenland ice core record, show decreased denitrification during stadials and the Younger Dryas. This suggests weaker productivity during stadials which the authors interpret as evidence of a weaker monsoon. Our model does not account for denitrification but lower productivity during a weak monsoon supports the authors posit of a weak monsoon-stadial link.

[29] *Gupta et al.* [2003] examined the percentage of a planktic foraminifer, *Globigerina bulloides*, in a core directly off Oman with centennial resolution through the Holocene. *G. bulloides* is usually a subpolar dwelling organism and can only live in the Arabian Sea due to strong cold upwelling. An increase in its percentage is interpreted as a strong monsoon and a decrease as a weak monsoon. According to our model results, the Oman core is indeed located in a region where a strong monsoon cools SSTs and hence the *Gupta et al.* [2003] interpretation is reasonable. It suggests, for example, a strong monsoon during the Medieval Climate Anomaly and a weak monsoon during the subsequent Little Ice Age. *Anderson et al.* [2002] used the same methodology (and some of the same data) and the same interpretation of the *G. bulloides* record to document the strengthening of the monsoon over the past four centuries, an interpretation that the modeling work here supports. It should be noted that the seasonal changes in SSTs are modest but the decadal to centennial timescale persistence of the monsoonal changes may still lead to an accumulation of the related signals. Furthermore, as mentioned in section 2, many of the paleostudies relate to periods with significantly different global climate in terms of the ice cover, SSTs, and winds. We expect that the impact over the Arabian Sea will still be felt through the imprint of these global climate signals on the seasonal cycle as appears to be the case in the anthropocene. Thus the paleorecords will only be amplified by the corresponding larger changes in monsoonal forcing and/or persistence of the seasonal changes over many decades and centuries.

[30] Earlier, *Naidu and Malmgren* [1996], examining climate change from the early to late Holocene showed that the percent abundance of *G. bulloides* in a core on the Oman margin was high during the early to mid-Holocene. This was a time of high northern summer insolation which would be expected to force a strong monsoon. According to the model results presented here, this would cause cool waters off Oman, consistent with the *G. bulloides* record.

[31] Farther south, *Charles et al.* [1997] examined a coral oxygen isotope record from the Seychelles (approximately 5°S and 55°W). They found that over the last 150 years positive values of the oxygen isotope ratio implied cold SSTs and were well correlated with strong monsoons. This is consistent with the model results in Figure 2. Wind speed effects are responsible for much of the cooling here during strong monsoons.

[32] Our results are, however, hard to reconcile with those of *Jung et al.* [2002]. They compared the oxygen isotope ratio of *G. bulloides* in a core off Somalia with the ratio in a stalagmite in Hoti Cave in Oman [*Neff et al.*, 2001]. The records covered the early to mid-Holocene. This comparison suggests that decadal to centennial periods of increased precipitation in Oman were times of warm waters off Somalia. In the current climate there is a weak positive relationship between Oman precipitation and summer monsoon precipitation over India (not shown). Consequently, on the basis of the models results presented here, these two records are incompatible. Further, *Jung et al.* [2002] claim that the oxygen isotope record implies variations of SST on decade to centennial timescales of 2–3 K which would require stronger variations in monsoon winds than occur in the current climate. Note also that the atmospheric response to the north of the Somali Jet axis and the ocean response within the strengthened jet may sequester different responses (R. Ramesh, personal communications, 2007) in addition to the potential nonstationarity of the correlation between Oman precipitation and Indian summer monsoons. Answering such details will require coupled climate experiments which are beyond the scope of this investigation.

[33] In summary, interpretations of sediment core proxies that relate evidence for cooler SSTs and/or higher productivity in the Arabian Sea to a stronger monsoon are on good ground. According to the model results presented here these relationships do hold up at the sites of the cores analyzed.

4.2. Summary

[34] The results essentially confirm the interpretation that has been consistently used for interpreting the paleoproxies that strong monsoons are preserved as biological responses to stronger coastal upwelling. Model results show that a stronger monsoon drives stronger upwelling along the west coast of the Arabian Sea but also surface cooling in the Arabian Sea. The impacts of monsoon variability are demonstrated as dynamical effects of wind stress forcing only and as wind stress plus wind speed effects. Including the wind speed effects clearly enhances the surface cooling both in the coastal upwelling region and in the open ocean all the way to the west coast of India and into the Bay of Bengal. Wind stress curls in the open ocean favor downwelling during strong monsoons leading to a deeper thermo-

cline and also deeper mixed layers leading to entrainment cooling. It should be reemphasized that surface cooling in the Arabian Sea is dominantly controlled by ocean dynamics and that evaporative cooling is minimal despite the large increase in surface wind speeds during strong monsoon regimes. The observational evidence supports this model-based conclusion. The impact of this seemingly nonintuitive process must be considered in interpreting paleoproxies.

[35] In the coastal upwelling region, stronger upwelling and related shallowing of the mixed layer is counteracted by stronger surface turbulent kinetic energy and entrainment cooling. While the open ocean region cools in the mean, the variability of SST cooling is relatively small in terms of standard deviation of the SST differences between strong and weak monsoons. The cooling is not limited to the surface layer but extends down to at least 100 m. Despite the surface convergence driven by stronger negative wind stress curl during strong monsoons, the central Arabian Sea cools due to the convergence of colder surface waters and deepening of the mixed layer due to entrainment of colder subsurface waters. Thus the traditional interpretation that strong monsoons drive evaporative cooling in the Arabian Sea is not supported by our model experiments. The implication of this for ecosystem response, especially in terms of salinity signatures in coral proxies, needs to be investigated with this in mind.

[36] The ecosystem response is investigated by contrasting the strong and weak monsoon year responses over the period 1948–2003. The enhanced upwelling and the entrainment cooling have a counterpart in terms of an increased supply of nitrate and dissolved iron which lead to enhanced surface chlorophyll and primary production. Cooler SSTs retard the growth rates for both size classes of phytoplankton but overall primary production is increased nonetheless except in the coldest regions in the Gulf of Aden. Export fluxes are similarly affected leading to generally larger exports in the shelf regions of coastal upwelling and in the open ocean. It is clear that over extended periods of enhanced or weakened monsoons, the Arabian Sea does respond so as to leave a biogenic signal in ocean sediments, corals, and speleotherms. The impacts of species succession in the coastal upwelling vs. the open ocean do not seem to affect the basic interpretations significantly. While this modeling study is more of a consistency check on the interpretation of the paleorecords in terms of the Arabian Sea response to monsoon variability, it does provide quantification to the surface cooling caused by coastal upwelling and open ocean entrainment cooling but with a negligible contribution from evaporative cooling. The impacts of precipitation and evaporation associated with these differences must be kept in mind in explaining past records or in designing future plans for gathering corals and sediment cores.

[37] **Acknowledgments.** R.M. thanks the NASA Indian Ocean mesoscale grant and the Scatterometer and Altimeter grants from NASA. Assistance from James Beauchamp is always invaluable. P.T. acknowledges postdoctoral scholarship from the Naval Research Laboratory.

References

Alexander, M. A., I. Bladé, M. Newman, J. R. Lanzante, N.-C. Lau, and J. D. Scott (2002), The atmospheric bridge: The influence of ENSO teleconnections on air-sea interactions over the global oceans, *J. Clim.*, *15*, 2205–2231.

Altabet, M., M. J. Higginson, and D. W. Murray (2002), The effect of millennial-scale changes in Arabian Sea denitrification on atmospheric CO_2, *Nature*, *415*, 159–162.

Anderson, D. M., J. T. Overpeck, and A. K. Gupta (2002), Increase in the Asian southwest monsoon during the past four centuries, *Science*, *297*, 596–599.

Annamalai, H., and R. Murtugudde (2004), Role of the Indian Ocean in regional climate variability, in *Earth Climate: The Ocean-Atmosphere Interaction*, *Geophys. Monogr. Ser.*, vol. 147, edited by C. Wang, S.-P. Xie and J. A. Carton, pp. 213–246, AGU, Washington, D. C.

Annamalai, H., J. Potemra, R. Murtugudde, and J. P. McCreary (2005), Effect of preconditioning on the extreme climate events in the tropical Indian Ocean, *J. Clim.*, *18*, 3450–3469.

Ballabrera-Poy, J., E. Hackert, R. Murtugudde, and A. J. Busalacchi (2007), An observation system simulation experiment for an optimal moored instrument array in the Indian Ocean, *J. Clim.*, *20*, 3284–3299.

Charles, C. D., D. E. Hunter, and R. G. Fairbanks (1997), Interaction between the ENSO and the Asian monsoon in a coral record of tropical climate, *Science*, *277*, 925–927.

Chen, D., L. Rothstein, and A. Busalacchi (1994), A hybrid vertical mixing scheme and its application to tropical ocean models, *J. Phys. Oceanogr.*, *24*, 2156–2179.

Christian, J. R., M. A. Verschell, R. Murtugudde, A. J. Busalacchi, and C. R. McClain (2002), Biogeochemical modeling of the tropical Pacific Ocean, I. Seasonal and interannual variability, *Deep Sea Res., Part II*, *49*, 545–565.

da Silva, A., A. C. Young, and S. Levitus (1994), Atlas of surface marine data 1994, vol. 1., Algorithms and procedures, *Tech. Rep. 6*, U.S. Dep. of Commer., NOAA, Natl. Environ. Satell., Data, and Inf. Serv., Silver Spring, Md.

Findlater, J. (1969), A major low-level air current near the Indian Ocean during northern summer monsoon, *Q. J. R. Meteorol. Soc.*, *95*, 362–380.

Giannini, A., R. Saravanan, and P. Chang (2003), Oceanic forcing of Sahel rainfall on interannual to interdecadal time scales, *Science*, *302*, 1027–1030.

Gupta, A. K., D. M. Anderson, and J. T. Overpeck (2003), Abrupt changes in the Asian southwest monsoon during the Holocene and their links to the North Atlantic Ocean, *Nature*, *421, 354–357.*

Han, W., J. P. McCreary, and K. E. Kohler (2001), Influence of P-E and Bay of Bengal rivers on dynamics, thermodynamics, and mixed-layer physics in the Indian Ocean, *J. Geophys. Res.*, *106*, 6895–6916.

Hoerling, M., and A. Kumar (2003), The perfect ocean for drought, *Science*, *299*, 691–694.

Ivanochko, T., R. Ganeshram, G.-J. Brummer, G. Ganssen, S. Jung, S. Moreton, and D. Kroon (2005), Variations in tropical convection as an amplifier of global climate change at the millennial-scale, *Earth. Planet. Sci. Lett.*, *235*, 302–314.

Jochum, M., and R. Murtugudde (2005), Internal variability of Indian Ocean SST, *J. Clim.*, *18*, 3726–3738.

Jung, S. J. A., G. R. Davies, G. Ganssen, and D. Kroon (2002), Decadal-centennial scale monsoon variations in the Arabian Sea during the early Holocene, *Geochem. Geophys. Geosyst.*, *3*(10), 1060, doi:10.1029/2002GC000348.

Kalnay, E., et al. (1996), The NCEP/NCAR 40–year reanalysis project, *Bull. Am. Meteorol. Soc.*, *77*, 437–471.

Kraus, E. B., and S. J. Turner (1967), A one-dimensional model of the seasonal thermocline. part II, *Tellus*, *19*, 98–105.

Levitus, S., J. I. Antonov, T. P. Boyer, and C. Stephens (2000), Warming of the world ocean, *Science*, *287*, 2225–2229.

Lighthill, M. J. (1969), Dynamic response of the Indian Ocean to the onset of the southwest monsoon, *Philos. Trans. R. Soc. London, Ser. A*, *265*, 45–92.

McCreary, J. P., P. K. Kundu, and R. Molinari (1993), A numerical investigation of dynamics, thermodynamics and mixed-layer processes in the Indian Ocean, *Prog. Oceanogr.*, *31*, 181–244.

McCreary, J. P., K. E. Kohler, R. R. Hood, and D. B. Olson (1996), A four-component ecosys-

tem model of biological activity in the Arabian Sea, *Prog. Oceanogr.*, *37*, 117–165.

Morey, S. L., M. A. Bourassa, X. J. Davis, J. J. O'Brien, and J. Zavala-Hidalgo (2005), Remotely sensed winds for episodic forcing of ocean models, *J. Geophys. Res.*, *110*, C10024, doi:10.1029/2004JC002338.

Murtugudde, R., and A. J. Busalacchi (1998), Salinity effects in tropical oceans, *J. Geophys. Res.*, *103*, 3283–3300.

Murtugudde, R., and A. J. Busalacchi (1999), Interannual variability of the dynamics and thermodynamics of the Indian Ocean, *J. Clim.*, *12*, 2300–2326.

Murtugudde, R., R. Seager, and A. Busalacchi (1996), Simulation of tropical oceans with an ocean GCM coupled to an atmospheric mixed layer model, *J. Clim.*, *9*, 1795–1815.

Murtugudde, R., A. J. Busalacchi, and J. Beauchamp (1998), Seasonal-to-interannual effects of the Indonesian throughflow on the tropical Indo-Pacific basin, *J. Geophys. Res.*, *103*, 21,245–21,441.

Murtugudde, R., S. Signorini, J. Christian, A. Busalacchi, C. McClain, and J. Picaut (1999), Ocean color variability of the tropical Indo-Pacific basin observed by SeaWiFS during 1997–1998, *J. Geophys. Res.*, *104*, 18,351–18,366.

Murtugudde, R., J. P. McCreary, and A. J. Busalacchi (2000), Oceanic processes associated with anomalous events in the Indian Ocean with relevance to 1997–1998, *J. Geophys. Res.*, *105*, 3295–3306.

Murtugudde, R., J. Beauchamp, C. McClain, M. Lewis, and A. Busalacchi (2002), Effects of penetrative radiation on the upper tropical ocean circulation, *J. Clim.*, *15*, 470–486.

Naidu, P. D., and B. A. Malmgren (1996), A high-resolution record of late Quaternary upwelling along the Oman Margin, Arabian Sea based on planktonic foraminifera, *Paleoceanography*, *11*, 129–140.

Neff, U., S. J. Burns, A. Mangini, M. Mudelsee, D. Fleitmann, and A. Matter (2001), Strong coherence between solar variability and the monsoon in Oman between 9 and 6 kyr ago, *Nature*, *411*, 290–293.

Overpeck, J., D. Anderson, S. Trumbore, and W. Prell (1996), The southwest Indian monsoon over the last 18000 years, *Clim. Dyn.*, *12*, 213–225.

Price, J. F., R. A. Weller, and R. Pinkel (1986), Diurnal cycling: Observations and models of the upper ocean response to diurnal heating, cooling, and wind mixing, *J. Geophys. Res.*, *91*, 8411–8427.

Rao, R. R., and R. Sivakumar (2000), Seasonal variability of near-surface thermal structure and heat budget of the mixed layer of the Indian Ocean from a new global ocean temperature climatology, *J. Geophys. Res.*, *105*, 995–1015.

Reynolds, R. W., and T. M. Smith (1994), Improved global sea surface temperature analyses, *J. Clim.*, *7*, 929–948.

Saji, N. H., B. N. Goswami, P. N. Vinayachandran, and T. Yamagata (1999), A dipole mode in the tropical Indian Ocean, *Nature*, *401*, 360–363.

Schott, F., and J. P. McCreary (2001), The monsoon circulation of the Indian Ocean, *Prog. Oceanogr.*, *51*, 1–123.

Schulz, H., U. von Rad, and H. Erlenkeuser (1998), Correlation between Arabian Sea and Greenland climate oscillations of the past 110,000 years, *Nature*, *393*, 54–57.

Seager, R., B. Blumenthal, and Y. Kushnir (1995), An advective atmospheric mixed layer model for ocean modeling purposes: Global simulation of surface heat fluxes, *J. Clim.*, *8*, 1951–1964.

Shukla, J., and M. Misra (1977), Relationship between sea surface temperature and wind speed over the central Arabian Sea and monsoon rainfall over India, *Mon. Weather Rev.*, *105*, 998–1002.

Vecchi, G. A., S.-P. Xie, and A. S. Fischer (2004), Ocean-atmosphere covariability in the western Arabian Sea, *J. Clim.*, *17*, 224–1213.

Vinayachandran, P. N. (2004), Summer cooling of the Arabian Sea during contrasting monsoons, *Geophys. Res. Lett.*, *31*, L13306, doi:10.1029/2004GL019961.

Wang, X., J. R. Christian, R. Murtugudde, and A. J. Busalacchi (2006), Spatial and temporal variability of the surface water pCO_2 and air-sea CO_2 flux in the equatorial Pacific during 1980–2003: A basin-scale carbon cycle model, *J. Geophys. Res.*, *111*, C07S04, doi:10.1029/2005JC002972.

Weare, B. C. (1979), A statistical study of the relationship between ocean surface temperatures and the Indian monsoon, *J. Atmos. Sci.*, *36*, 2279–2291.

Webster, P. J., V. Magaña, T. N. Palmer, J. Shukla, R. A. Tomas, M. Yanai, and T. Yasunari (1998), Monsoons: Processes, predictability and the prospects for prediction, *J. Geophys. Res.*, *103*, 14,451–14,510.

Webster, P. J., A. M. Moore, J. Loschnigg, and R. R. Leben (1999), Coupled ocean-atmosphere dynamics in the Indian Ocean during 1997–98, *Nature*, *401*, 356–360.

Wiggert, J. D., R. Murtugudde, and C. R. McClain (2002), Processes controlling interannual variations in wintertime (northeast monsoon) primary productivity in the central Arabian Sea, *Deep Sea Res., Part II*, *47*, 2319–2343.

Wiggert, J. D., R. Murtugudde, and J. R. Christian (2006), Annual ecosystem variability in the tropical Indian Ocean: Results of a coupled bio-physical ocean general circulation model, *Deep Sea Res., Part II*, *53*, 644–676.

Winguth, A. M. E., M. Heimann, K. D. Kurz, E. Maier-Reimer, U. Mikolajewicz, and J. Segschneider (1994), El Niño–Southern Oscillation related fluctuations of the marine carbon cycle, *Global Biogeochem. Cycles*, *8*, 39–64.

R. Murtugudde, Earth System Science Interdisciplinary Center, 2201 Computer and Space Sciences Building, University of Maryland, College Park, MD 20742, USA. (ragu@essic.umd.edu)

R. Seager, Physical Oceanography, Lamont-Doherty Earth Observatory, Columbia University, Route 9W, Palisades, NY 10964, USA.

P. Thoppil, Department of Marine Sciences, University of Southern Mississippi, Code 7320, Stennis Space Center, MS 39529, USA.